



1 **Manganese incorporation in living (stained) benthic foraminiferal**
2 **shells: A bathymetric and in-sediment study in the Gulf of Lions**
3 **(NW Mediterranean).**

4 Shauna Ní Fhlaithearta¹, Christophe Fontanier^{2, 3, 4}, Frans Jorissen⁴, Aurélie Mouret⁴,
5 Adriana Dueñas-Bohórquez¹, Pierre Anschutz², Mattias B. Fricker⁵, Detlef Günther⁵,
6 Gert J. de Lange¹, Gert-Jan Reichart^{1, 6}

7

8 ¹ Faculty of Geosciences, Utrecht University, Utrecht, The Netherlands.

9 ² EPOC, UMR CNRS 5805, University of Bordeaux, Pessac, France

10 ³ FORAM, Foraminiferal Study Group, F-29200, Brest, France

11 ⁴ Université d'Angers, LPG-BIAF, UMR CNRS 6112, 49045 Angers Cedex, France

12 ⁵ Laboratory of Inorganic Chemistry, ETH Zurich, 8093 Zurich, Switzerland.

13 ⁶ Royal NIOZ, Texel, The Netherlands

14

15 Corresponding author: S. Ni Fhlaithearta, s.ni.fhlaithearta@gmail.com

16 Keywords: Benthic foraminifera, minor/trace metals, calibration study, Gulf of Lions, Mn/Ca

17

18 **Abstract**

19 Manganese geochemistry in deep-sea sediments is known to vary greatly over the first
20 few centimeters, which overlaps with the in-sediment depth habitats of several benthic
21 foraminiferal species. Here we investigated manganese incorporation in benthic
22 foraminiferal shell carbonate across a 6-station depth transect in the Gulf of Lions,
23 NW Mediterranean to unravel the impacts of foraminiferal ecology and Mn pore
24 water geochemistry. Over this transect water depth increases from 350 to 1987 m,
25 while temperature (~13°C) and salinity (~38.5) remained relatively constant.
26 Manganese concentrations in the tests of living (Rose Bengal stained) benthic
27 foraminiferal specimens of *Hoeglundina elegans*, *Melonis barleeanus*, *Uvigerina*
28 *mediterranea*, *Uvigerina peregrina* were measured using laser ablation inductively
29 coupled mass spectrometry (laser ablation ICP-MS). Pore water manganese
30 concentrations show a decrease from shallow to deeper waters, which corresponds to



31 a generally decreasing organic matter flux with water depth. Differences in organic
32 matter loading at the sediment water interface affects oxygen penetration depth into
33 the sediment and hence Mn pore water profiles. Mn/Ca values for the investigated
34 foraminiferal species reflect pore water geochemistry and species-specific
35 microhabitat in the sediment. The observed degree of variability within a single
36 species is in-line with know ranges in depth habitat and gradients in redox conditions.
37 Both Mn/Ca ratio and inter-specific variability hence reflect past Mn cycling and
38 related early diagenetic processes within the sediment, making this a potential tool for
39 bottom-water oxygenation and organic-matter fluxes. Dynamics of both in-sediment
40 foraminiferal depth habitats and Mn cycling, however, limit the application of such a
41 proxy to settings with relatively stable environmental conditions.

42

43 **1. Introduction**

44

45 Reconstructing past climate and environmental change largely depends on so-called
46 proxies. These proxies relate measurable variables in the geological record to target
47 parameters, such as e.g. temperature, biological productivity and bottom water
48 oxygenation. The carbonate shells of unicellular protists, foraminifera, are one of the
49 most utilized signal carriers for reconstructing past environments. Both the census
50 data of foraminifera and the geochemical composition of the shells are used in this
51 context. The geochemical composition of the shells is investigated for their stable
52 isotopic composition as well as for their trace and minor element incorporation. Both
53 surface and bottom water conditions are reconstructed this way, using planktonic and
54 benthic foraminiferal species respectively.

55 Most existing calibrations of trace element uptake in foraminiferal test
56 carbonate are based on comparing their composition with bottom water conditions



57 (Elderfield et al., 2006; Nürnberg et al., 1996; Yu and Elderfield, 2007). Many
58 benthic foraminiferal species live, however, within the sediment and precipitate their
59 calcium carbonate test in contact with pore water. As a result, the trace metal
60 composition of pore water exerts a control on the uptake of trace metals in their test.
61 This effectively links benthic foraminiferal microhabitat preference and pore water
62 chemistry. On the one hand, this creates complications when using foraminiferal trace
63 metal ratios for reconstructing bottom water conditions, whereas on the other hand, it
64 offers the possibility to develop proxies of pore water chemistry in the past.

65 Linking foraminiferal test chemistry with pore water chemistry requires in-
66 depth knowledge of, 1) how early diagenesis in sediments affects pore water
67 chemistry, 2) the habitat preference of the foraminiferal species, 3) foraminiferal
68 migration (and calcification) within the uppermost sediment layer. In principle, the
69 chemical composition of living (stained) benthic foraminifera will reflect all these
70 processes.

71 For many elements an important inter-specific difference in uptake of trace
72 metals has been observed (Hintz et al., 2006; Wit et al., 2012), a so-called vital effect.
73 This implies that in addition to ecology and pore water geochemistry, trace metal
74 partitioning also needs to be taken into consideration. This requires a comparative
75 study between locations where all three of these aspects have been quantified.

76 Reconstructing past pore water trace metal profiles is important since it
77 provides valuable information on organic carbon degradation and recycling of
78 nutrients at the seafloor (Van Cappellen and Wang, 1996; De Lange, 1986). Such
79 diagenetically controlled trace metal profiles are used in quantitative models
80 constraining oceanic carbon fluxes and burial (Wang and Van Cappellen, 1996).



81 Knowledge of such profiles in the past could thus help to reconstruct past carbon
82 cycles.

83 Benthic foraminiferal species have a specific preference for their depth-habitat
84 (Jorissen et al., 1995). Some benthic foraminiferal species are limited to a very narrow
85 environmental in-sediment range, for example, along redox fronts, whereas others
86 have a wider distribution, thriving under variable conditions and consequently occupy
87 a broader niche. These differences in depth-habitat preferences could be related to the
88 presence of different types of metabolism (Koho et al., 2011; Risgaard-Petersen et al.,
89 2006). As such, trace metal profiles and foraminiferal in-sediment depth habitat can
90 be related, such as recently proposed in a conceptual (TROXCHEM³) model for the
91 redox sensitive element, manganese, by Koho et al. (2015). Studying the interplay
92 between benthic foraminiferal habitat preference and incorporation of redox-sensitive
93 trace elements is key to verifying such models.

94 Studying manganese bound in foraminiferal shell carbonate lies at the
95 intersection of foraminiferal ecology and early diagenesis in sediments. Manganese is
96 a redox sensitive element and exists as Mn- (hydr)oxides in the presence of oxygen.
97 As oxygen concentrations in the sediment decreases due to ongoing organic matter
98 remineralization, Mn-(hydr)oxides are reduced to aqueous Mn²⁺, (Froelich et al.,
99 1979). Manganese in sediments cycles continuously between solid and aqueous state
100 as a result of upward diffusion of Mn²⁺ and consequent remineralization to Mn-
101 (hydr)oxides. Hence proxy studies must account for both ecological controls, like
102 foraminiferal habitat preference, as well as geochemical controls like oxygen
103 concentrations and organic matter loading (Glock et al., 2012; Groeneveld and
104 Filipsson, 2013; Koho et al., 2015, 2017; McKay et al., 2015; Reichart et al., 2003).
105 Notably, both benthic foraminifera and trace metal geochemistry react to organic



106 matter recycling and bottom water oxygenation (Jorissen et al., 1995). This implies
107 that locations with contrasting conditions, both low and high bottom-water
108 oxygenation as well as low and high productivity, are required for testing. Whereas
109 most of these studies focused on the role of bottom water oxygenation in relatively
110 oxygen poor settings, here we focus on the well-oxygenated western Mediterranean.

111 In this study we combine pore water geochemistry, foraminiferal habitat
112 preference and test geochemistry in an area characterized by well-oxygenated bottom
113 water conditions and average productivity. Results are compared with earlier studies
114 from high productivity regimes and low-oxygen conditions at the sediment-water
115 interface (e.g. Arabian Sea, Koho et al., 2015 and Mediterranean sapropel deposition,
116 Ní Fhlaithearta et al., 2010). Specifically, we investigate the link between manganese
117 incorporation and benthic foraminiferal ecology and compare this to the recently
118 proposed TROXCHEM³ model (Koho et al., 2015). Four species of living (stained)
119 foraminifera were sampled along a 6-station bathymetric transect in the Gulf of Lions,
120 NW Mediterranean. Individuals were picked from a series of in-sediment depths and
121 analyzed by laser ablation ICP-MS, enabling multiple analyses of single specimens.

122

123 **2. Material and methods**

124

125 **2.1 Study area and sediment sampling**

126 Cores were collected with a classical Barnett multicorer (Barnett et al. 1984) at 6
127 stations in the Gulf of Lions (NW Mediterranean) during the August-September 2006
128 BEHEMOTH cruise (Fig. 1, Table 1). The 6 stations describe a bathymetric transect
129 from 350m to 1987m depth. The shallowest site, station F, is bathed in Mediterranean
130 Intermediate Water (MIW). Stations E (552 m) and D (745 m) are positioned at the



131 transition of MIW and Western Mediterranean Deep Water (WMDW). Stations C
132 (980 m), B (1488 m) and A (1987 m) are bathed by the WMDW. Bottom water
133 temperature is stable through the part of the water column studied here (~13.1°C)
134 (Xavier Durrieu de Madron, pers. com.). Salinity ranges between 38.4 and 38.5. The
135 multicorer allowed sampling of the first decimeters of the sediment, the overlying
136 bottom waters, and an undisturbed sediment-water interface. Cores were sliced for
137 foraminiferal studies with a 0.5-cm resolution down to 4 cm, followed by 1 cm slices
138 down to 10 cm depth. Sediments were put in an ethanol-Rose Bengal mixture (95%
139 ethanol with 1g/l Rose Bengal), in order to identify living (stained) specimens. For
140 more detailed information about methods, please consult Fontanier et al., (2008).

141

142

143 **2.2 Pore water geochemistry**

144 Sediment sampling for pore water extraction was carried out under an inert
145 atmosphere (N₂). Hereafter, samples were centrifuged at 3500 rpm for 20 min. The
146 supernatant was filtered and acidified (HNO₃ *s.p.*) for analyzing dissolved metals.
147 Dissolved Mn concentrations were determined with flame atomic absorption
148 spectrometry (Perkin Elmer AA 300). Precision for this method is ± 5%. A pore water
149 subsample was also analyzed for Mn using ICP-MS (Agilent 7500 Series). Relative
150 precision for this method is 3%. Total alkalinity of pore water was measured at
151 Utrecht University using an automated titrator (702 SM Titrino, Metrohm) making
152 Gran plots. Dissolved Inorganic Carbon (DIC) was measured using a Dissolved
153 Carbon Analyser (Shimadzu, Model TOC-5050A). Carbonate ion concentrations were
154 calculated using the CO2SYS software (version 01.05; Lewis and Wallace, 1998).



155 Analytical uncertainty for the alkalinity is about 10 μeq , relative standard deviation
156 for the DIC analyses is 0.8%.

157 Oxygen concentration profiles were determined using Clark-type
158 microelectrodes (Unisense©, Denmark). Labile organic matter was derived from the
159 sum of lipids, amino acids and sugars measured in the top cm of sediment; for details,
160 see Fontanier et al., 2008.

161

162 **2.3 Foraminiferal trace metal geochemistry**

163 Foraminiferal trace element concentrations were determined using two laser ablation
164 ICP-MS systems. Prior to laser ablation, all samples were gently cleaned in methanol
165 (x1) and UHQ water (x4). Between each rinse, the samples were placed in a sonic
166 bath for several seconds to thoroughly clean the tests. Benthic foraminifera from 745
167 m (station D), 980 m (station C), 1488 m (station B) and 1987 m (station A) were
168 measured at Utrecht University using a deep UV (193nm) ArF excimer laser (Lambda
169 Physik) with GeoLas 200Q optics. Ablation was performed at a pulse repetition rate
170 of 10 Hz, and energy density of 1.4 J/cm², with a crater size of 80 μm . Ablated
171 particles were measured by a quadrupole ICP-MS (Micromass Platform) equipped
172 with a collision and reaction cell. Such a collision and reaction cell improves
173 carbonate analyses by eliminating interferences on mass 44. Scanned masses included
174 ²⁴Mg, ²⁶Mg, ²⁷Al, ⁴²Ca, ⁴³Ca, ⁵⁵Mn, ⁸⁸Sr, ¹³⁷Ba, ¹³⁸Ba, ²⁰⁸Pb. Benthic foraminifera
175 from stations F (350 m) and E (552 m) were analyzed at ETH-Zurich (due to
176 laboratory renovations at Utrecht University). The laser type and ablation parameters
177 were identical to those detailed above. The ablated particles were measured using a
178 quadrupole ICP-MS (ELAN 6100 DRC, Perkin-Elmer). In both cases, calibration was
179 performed using an international standard (NIST610) with Ca as an internal standard



180 (Jochum et al. 2011). The same masses as measured in Utrecht were monitored, in
181 addition to ^7Li , ^{23}Na , ^{47}Ti , ^{60}Ni , ^{61}Ni and ^{89}Y . Inter-laboratory compatibility was
182 monitored using a matrix-matched calcite standard.

183 Analytical error (equivalent to 1 sigma), based on repeated measurement of an
184 external standard, was <5% for reported elements. Each laser ablation measurement
185 was screened for contamination by monitoring Al and Pb. On encountering surface
186 contamination, the data integration interval was adjusted to exclude any Al or Pb
187 enrichment. Cross-plots between Al and Pb versus Mn showed that they are unrelated,
188 confirming accuracy of the integrations.

189 During the laser ablation analyses the different trace elements were monitored
190 with respect to time, thus representing a cross section of the test wall. This allows not
191 only quantification of the different trace metals of interest, but also to observe
192 variability within individual tests. Each species has a distinct test-wall thickness,
193 permitting the study of intra-test variability. A typical ablation profile for *H. elegans*
194 is shown in Fig. 2.

195

196 **2.4 Analyses of manganese in foraminiferal tests**

197 Contamination and presence of secondary Mn-rich coatings on benthic foraminiferal
198 tests has been a longstanding challenge in trace metal analyses of benthic foraminifera
199 (Boyle 1983, Lea and Boyle 1989). In this study the trace metal data are based
200 exclusively on living (Rose Bengal stained) foraminifera, which effectively rules out
201 the impact of Mn-rich coatings on trace metal concentrations. At the time of sampling,
202 the collected tests were still enveloped by foraminiferal cytoplasm, preventing the
203 formation of extraneous inorganic precipitates. Although benthic foraminifera live
204 within the sediment, their test is physically separated from the environment as they



205 are enveloped in an organic sheath (Ni Fhlaithearta et al., 2013). In case a recently
206 deceased foraminifer was mistakenly analyzed (still with sufficient protoplasm to
207 stain with Rose Bengal) the Mn oxide would not only have had limited time to
208 develop, but it would also show up as a Mn spike at the start of a laser ablation profile.
209 The ablation profiles confirm that no Mn-rich phases are present at the test surfaces
210 (Fig. 2).

211 Comparing LA-ICP-MS data with traditional solution analyses for
212 foraminiferal Mg/Ca values showed that data are directly comparable (Rosenthal et al.,
213 2011). Also for trace metals such as Ni²⁺, Cu²⁺ and Mn²⁺, cross-calibration of LA-
214 ICP-MS and micro-XRF shows those analytical results are robust (Munsel et al.,
215 2010).

216

217 **2.5 Benthic foraminiferal Mn/Ca**

218 Manganese incorporation in benthic foraminiferal test carbonate was analyzed from 4
219 different species (*Hoeglundina elegans*, *Melonis barleeanus*, *Uvigerina mediterranea*,
220 *Uvigerina peregrina*), from 6 coring sites, for up to 9 depths in the sediment. Sample
221 coverage for all stations is described in Table 2. Descriptive statistics are presented in
222 Table 3.

223

224 **2.5.1 Intra-individual variability**

225 From the largest taxon, *Uvigerina mediterranea*, 3-4 analyses were routinely carried
226 out per test, and no trend in Mn/Ca values was seen in consecutive growth stages.
227 From the other species two analyses were performed per test. The resolution of the
228 ablation profiles themselves does not allow quantifying changes in trace metals within
229 the test wall. Still, comparing the data within individual ablation profiles shows that



230 the intratest variability is generally limited for Mn (Table 4). As the ablation profiles
231 target one chamber mostly, this does not include the full potential range. Comparing
232 different ablation profiles between chambers in a single shell would circumvent this,
233 but this data is somewhat limited.

234

235 **2.5.2 Distribution characteristics of Mn/Ca in benthic foraminiferal calcite**

236 Boxplots are used to describe the range of Mn/Ca values and how the distribution,
237 median, average and skewness compares between species.. All ICP-MS
238 measurements are included, and as such represent both intra- and inter-individual
239 variation.

240

241 **3. Results**

242 **3.1 Pore water data**

243 Pore water dissolved manganese (Mn^{2+}) concentrations were measured at all six
244 stations. Manganese concentrations increase below the oxygen penetration depth at
245 stations C and D (Fig. 3), with the highest in-sediment Mn^{2+} concentrations reached at
246 station D. At stations E and F manganese concentrations remain low after crossing the
247 oxygen penetration depth. At stations A and B the oxygen penetration depth and
248 MnO_2/Mn^{2+} redox boundary are deeper than 10 cm's. Dissolved inorganic carbon
249 (DIC) and total alkalinity (TA), were measured at stations E, C and B (Fig. 4). At
250 stations D, C and E, DIC concentrations in the top 10 cm have a similar range (2350-
251 2700 $\mu\text{mol/kg}$). The DIC profile at station B has a narrower range, ranging from
252 2400-2550 $\mu\text{mol/kg}$. Total alkalinity values range from 3242 $\mu\text{mol/kg}$ at station E to a
253 minimum of 2774 at station B. Carbonate ion concentrations [CO_3^{2-}] were derived
254 based on TA and DIC values. The [CO_3^{2-}] profiles were relatively similar (Fig. 4) for



255 stations E and C and B. Values for all three stations ranged from a maximum of 419
256 $\mu\text{mol/kg}$ at station E to a minimum of 192 $\mu\text{mol/kg}$ at station C (Fig. 4).

257 **3.2 Mn/Ca data**

258 **3.2.1 Intra-individual variability**

259 For most species some Mn/Ca analyses were below detection limit, except for *M.*
260 *barleeanus*, which contained measurable quantities of Mn in all shells analyzed. This
261 was most evident for *H. elegans*, where all but three Mn/Ca measurements were
262 below detection limit (dl). *Uvigerina peregrina* had a wider range of Mn/Ca values
263 than *U. mediterranea*. *Melonis barleeanus* exhibited the largest range of Mn/Ca
264 values of the four studied species (Fig. 5). For all species, except *H. elegans*, values
265 are somewhat skewed towards higher values.

266

267 **3.2.3 Foraminiferal Mn/Ca variation across a depth transect**

268 A trend of decreasing manganese incorporation with increasing water depth (350-
269 1987 m) is most clearly visible in *M. barleeanus* (Fig. 6), except that the maximum
270 values are observed at station E at 552 m. *Melonis barleeanus* shows the highest
271 Mn/Ca values and the largest Mn/Ca variability. Station E registers the broadest
272 Mn/Ca variability, which decreases with increasing water depth. *U. peregrina* also
273 exhibits the largest variability in Mn/Ca values at station E. For *U. peregrina*, Mn^{2+}
274 incorporation decreases from 350 m to 1987 m, except for station D (745 m), where
275 Mn/Ca values (between the 10 – 90th percentile) are approximately equivalent to those
276 at station A (350 m; Fig. 6). For *U. mediterranea* a trend of decreasing Mn
277 incorporation with increasing depth is found in specimens of *U. mediterranea* from
278 the sediments at 552, 745 and 980 m. The highest values are reached at the shallowest
279 station (350 m). Station E is also marked by the highest minimum Mn/Ca values for *U.*



280 *mediterranea*. At station A only two *U. mediterranea* measurements are above the
281 detection limit. *Hoeglundina elegans* shells from three stations (350 m, 1488 m and
282 1987 m) were analyzed, however, all but three measurements were below detection
283 limit (Fig. 6). These slightly elevated values were recorded at the shallowest station
284 (station F). These Mn/Ca values are still very low compared to ranges in Mn/Ca
285 values observed for the other species (Fig. 6).

286 Variability in Mn/Ca increases together with the overall Mn/Ca concentration
287 within benthic foraminiferal species (Table 4). This suggests that even at those
288 stations and depth levels where the highest Mn concentrations are recorded,
289 individuals with relatively low amounts of Mn in their calcitic test were found.
290 Comparing relative standard deviations, as a measure for the inter-specimen
291 variability, for the different stations and species suggests that with increasing Mn
292 concentration for *M. barleeanus* and *U. mediterranea* variability increases, whereas
293 for *U. peregrina* it decreases.

294

295 **3.2.4 In-sediment variation**

296 For most species Mn/Ca values are more or less constant with in-sediment depth (Fig.
297 3). However, *M. barleeanus* shows increasing Mn/Ca values with in-sediment depth.
298 This is most apparent at the shallowest station (station F - 350 m) (Fig. 3d).

299

300 **4. Discussion**

301

302 Incorporation of Mn in benthic foraminiferal carbonate depends both on foraminiferal
303 ecology and early diagenesis in sediments. Although other factors such as temperature,
304 sea water carbonate chemistry, growth rate etc., might also affect the uptake of Mn in



305 the shell carbonate (Koho et al., 2017), these effects are most likely several orders of
306 magnitude smaller compared to the large range in dissolved Mn in pore water. Since
307 pore water Mn is the dominant factor controlling Mn incorporation, studies must
308 account for ecological controls, like foraminiferal depth habitat preference, as well as
309 for geochemical controls like oxygen concentrations and organic matter fluxes (Koho
310 et al., 2015; De Lange, 1986; Reichart et al., 2003).

311

312 **4.1 Impact of redox conditions and foraminiferal habitat preference** 313 **on Mn incorporation**

314 In general, flux of organic matter arriving at the sea floor decreases with increasing
315 water depth, due to ongoing degradation during settling (Arndt et al., 2013 and
316 references therein). Consequently, redox boundaries within the sediment generally
317 also deepen as a function of water depth, as oxygen consumption in the sediment
318 decreases. Such a fundamental organic matter-depth relation is in line with the much
319 deeper oxygen penetration depths at stations A and B compared to the more shallow
320 stations. At station F the relative shallow oxygen penetration depth observed is in line
321 with its' relative shallow water depth, although the organic matter which arrives here
322 at the seafloor apparently undergoes winnowing (Fontanier et al., 2008). The organic
323 matter along the transect studied is concentrated at a so-called depocenter, which
324 largely coincides with the depths of stations C and D (Fontanier et al., 2008). As
325 bottom waters at all stations are well oxygenated, organic matter concentration can be
326 considered the main control for redox conditions at stations F-A, with the amount of
327 organic matter arriving at the seabed being regulated by water depth and sedimentary
328 processes, such as focusing versus winnowing.



329 At stations C, D and F, the oxygen penetration depth and the Mn^{2+} redox
330 boundaries are at the same depth, as expected. Station F shows the shallowest OPD of
331 all stations, although the organic matter concentration is relatively low. One
332 explanation for this observation is that a lower porosity at F (56% versus 76% and
333 79 % at stations D and E, respectively) impedes oxygen diffusion through the
334 sediment. Alternatively, the pore water profile reflects an earlier organic matter
335 deposition event, with this organic matter being largely consumed at the time of
336 sampling. The pore water profiles require more time to re-equilibrate to the new
337 conditions (Burdige and Gieskes, 1983). At station E there is a mismatch between
338 oxygen penetration depth and the Mn^{2+} redox boundary as the Mn^{2+} redox boundary is
339 considerably deeper than the OPD. Although this is in line with the observed higher
340 bioirrigation at this station (Fontanier et al., 2008), this might reflect non-equilibrium
341 conditions as well.

342 The vertical distribution of benthic foraminiferal species varies between
343 stations, in accordance with organic matter concentrations and redox zonation, which
344 is consistent with the TROX model (Jorissen et al., 1995; Fontanier et al., 2008). In
345 case of a shallower redox zone, infaunal benthic foraminifera biomineralize in contact
346 with Mn-enriched pore water, with highest dissolved manganese concentrations
347 occurring just below the oxygen penetration depth at all stations, except for station E
348 (552 m). This is in contrast to low bottom-water oxygen environments often studied in
349 the context of proxy development studies, where pore water Mn^{2+} is released from the
350 pore water (Koho et al., 2015, 2017; Mangini et al., 2001).

351 The species studied here cover the range of shallow-infauna to intermediate-
352 infauna niches. *Hoeglundina elegans*, a typically shallow infaunal species, is often
353 found close to the sediment-water interface (Jorissen et al., 1998; Schönfeld 2001;



354 Fontanier et al., 2002; Fontanier et al., 2008) and contains the lowest concentration of
355 Mn in its test. Only at the shallowest station (350 m) three specimens of *H. elegans*
356 show concentrations above the detection level, with values still low compared to the
357 values observed for the other species (Fig. 6). In the Bay of Biscay Reichart et al.
358 (2003) also suggested that elevated Mn concentrations in *H. elegans* were confined to
359 stations with oxygen depleted bottom waters and/or with a shallow oxygen
360 penetration depth. *Uvigerina mediterranea* and *Uvigerina peregrina* are also classed
361 as shallow-infaunal species; they are typically found within the top few centimeters of
362 the sediment column (Fontanier et al. 2002, Fontanier et al. 2008). The calculated
363 average living depth (ALD₁₀) as calculated in Fontanier et al. (2008) is consistently
364 shallower than the ALD₁₀ for *U. mediterranea*. This is at odd with previous reports
365 suggesting *U. peregrina* has a slightly deeper microhabitat than *U. mediterranea*
366 (Fontanier et al. 2002; 2006). That *U. peregrina* has a deeper microhabitat is further
367 supported by the usual distinct $\delta^{13}\text{C}$ offset in *U. peregrine*, which is more depleted
368 compared to *U. mediterranea* (Schmiedl et al., 2004; Fontanier et al, 2002, 2006). The
369 higher Mn/Ca values observed here for *U. peregrina* (Figure 6) supports the idea that
370 it calcifies somewhat deeper in the sediment compared to *U. mediterranea*.
371 Alternatively, *U. peregrina* may migrate downwards within burrows to track food
372 resources, recording redox steepness (Loubere et al., 1995). This could highlight a
373 disparity between the assumed living depth (the depth interval of recovery) and
374 biomineralization depth of foraminifera. Still, this would also result in a higher
375 variability of Mn/Ca values at higher Mn/Ca levels, which is not observed. Hence,
376 more likely the observed disparity between the geochemical signals incorporated into
377 foraminiferal calcite and depth of recovery in *U. peregrina* reflects opportunistic
378 behaviour, with calcification at a shallower in-sediment depth in response to more



379 favourable conditions after e.g. seasonal peaks in organic matter fluxes (Accornero et
380 al., 2003), when the OPD is close to the sediment water interface.

381 *Melonis barleeanus*, generally considered an intermediate-infaunal species
382 (Fontanier et al., 2002, 2008), contains the highest concentrations of Mn in its test.
383 Manganese incorporation in this species increases with increasing labile organic
384 matter (Fig. 7a).

385 In summary, the habitat preference of the benthic foraminiferal species studied
386 here is reflected in the Mn/Ca values recorded in their tests. This is in contrast with
387 other results showing lower Mn/Ca values in foraminiferal tests with shallower redox
388 fronts (Koho et al., 2015). This, however, critically depends on the Mn being released
389 to the water column, which only occurs when the bottom waters are disoxic. In case
390 of a seasonal organic matter deposition event, an increase of Mn concentration in
391 foraminiferal test carbonate would initially occur in the deeper and ultimately also in
392 the more shallow calcifying foraminifera. This is in line with the conceptual
393 TROXCHEM³ model, with the conditions studied here falling within the first stage of
394 the temporal succession considered in the model. Bottom water remains well
395 oxygenated (O₂ concentrations at the study area: 199-219 μmol/l (Fontanier et al.,
396 2008)) and organic matter loading is controlling Mn²⁺ concentrations in the sediment.
397 To what extent species are high in Mn/Ca depends on living depth and opportunistic
398 behavior.

399 At a given location, a benthic foraminiferal species' depth preference or
400 biomineralization depth, is reflected in its average Mn/Ca value (Fig. 5). The trend
401 across a depth transect shows a strong correlation to labile organic matter
402 concentrations in the surface sediments (Fig. 7). The strong correlation between labile
403 organic matter (i.e. sedimentary lipid content) and Mn incorporation in shallow and



404 intermediate infaunal species *U. mediterranea* ($R^2 = 0.80$ ($p < 0.05$)) suggests that test
405 Mn has potential as a proxy for detecting past labile organic matter fluxes. Notably,
406 *M. barleeanus* has a very strong correlation (0.81), though this correlation lacks
407 statistical significance ($p > 0.05$). In contrast, *U. peregrina* shows a correlation
408 coefficient of only 0.45 (R^2) between test Mn and labile organic matter. *Uvigerina*
409 *peregrina* is reported to respond opportunistically to the concentration and quality of
410 organic matter produced during bloom events (Fontanier et al., 2003; Koho et al.,
411 2008; Barras et al., 2010). This response is in the form of increased reproduction and
412 growth. Perhaps *U. peregrina* calcifies at shallow depths and therefore does not
413 capture the Mn^{2+} gradient.

414 At low oxygen concentrations Mn is released through the reduction of
415 manganese (oxy)hydroxides. Here we show an increase in Mn/Ca incorporation in
416 several species, from shallow to intermediate-depth infaunal habitats, as a function of
417 oxygen penetration depth. Such a correlation agrees with studies by Ní Fhlaithearta et
418 al. (2010) and McKay et al. (2015) from a down core record of Mn/Ca_{H. elegans} during
419 the formation of sapropel (S1) in the Eastern Mediterranean and a paleoproductivity
420 study of an upwelling system in the NE Atlantic, respectively. Here, a comparison of
421 Mn (oxy)hydroxides in the sediment and foraminiferal Mn^{2+} showed that Mn^{2+}
422 incorporation in an epifaunal to shallow infaunal species was higher during times of
423 enhanced Mn^{2+} remobilization and hence higher pore water Mn^{2+} . Such a correlation,
424 however, requires that the bottom waters remain somewhat oxygenated to retain the
425 dissolved Mn^{2+} in the pore water. With disoxic bottom waters Mn^{2+} escapes the
426 porewater and foraminiferal Mn/Ca values decrease (Koho et al., 2015). However,
427 with high organic matter deposition, which might be concentrated in events, also



428 foraminiferal species living at or close to the sediment water interface may show
429 elevated Mn concentrations.

430 In addition to the here observed changes, biomineralization could affect Mn^{2+}
431 incorporation. To date, however, no studies have been carried out under controlled
432 conditions to constrain species-specific offsets in Mn incorporation. In a controlled
433 laboratory study by Munsel et al (2010) Mn incorporation in *Ammonia tepida*
434 increased with increasing Mn^{2+} concentrations in the culture water and the partition
435 coefficient was well above 1. The lack of any appreciable discrimination argues
436 against a major biomineralization impact on Mn^{2+} partitioning. Also our data does not
437 suggest a major impact of biomineralization on Mn incorporation.

438 In summary, Mn incorporation seems primarily controlled by pore water
439 conditions in close proximity to the test, with a secondary control determined by the
440 ability of a foraminifer to seasonally calcify and migrate within the sediment.

441

442 **4.2 Pore water Mn dynamics and foraminiferal migration within the sediment**

443 Manganese is incorporated in foraminiferal carbonate with a partition coefficient (D)
444 close to 1 (Munsel et al., 2010), which argues for a minor biomineralization control.
445 We calculated Mn partition coefficients for *U. mediterranea*, *U. peregrina* and *M.*
446 *barleeanus* at stations E, C and B (Table 6) based on average Mn/Ca_{foram} and average
447 $Mn/Ca_{\text{pore water}}$ values found above the Mn^{2+} -MnO(H) redox boundary. Calculated D_{Mn}
448 agrees with the previously reported D_{Mn} by Munsel et al., (2010), with values varying
449 between ~1-2 for *U. mediterranea* and *U. peregrina*. The Mn partition coefficient for
450 *Melonis barleeanus* ranges from ~4-7. The partition coefficient for this species most
451 likely reflects its capacity to calcify under dysoxic conditions, close to or even below
452 the oxygen penetration depth. Still, this calculation is based on two assumptions: (1)
453 the depth foraminifera are recovered from during sampling corresponds with the



454 average depth of calcification and, (2) variation in pore water is limited. Establishing
455 species specific Mn partitioning coefficients using culture experiments might,
456 however, be needed for unlocking the full potential of this proxy.

457 A foraminifer calcifying within a steep Mn^{2+} gradient is exposed to a higher
458 range of Mn^{2+} concentrations (over a fixed depth interval) compared to specimens
459 living along a more gradual Mn^{2+} concentration gradient. Since foraminifera can
460 migrate through the sediment as a response to food availability and oxygen
461 concentrations (Alve and Bernhard 1995; Gross, 2000), not only the slope of the Mn
462 gradient, but also the in-sediment depth range (microhabitat) of the foraminifer in
463 relation to the Mn redox boundary, should be considered (Fig. 8). A shallow-infauna
464 species, with a limited in-sediment range, would be expected to exhibit lower
465 variability than an intermediate- infauna species, which possibly migrates
466 considerably in depth. This is exemplified at station F (350 m) where we note an
467 increase in foraminiferal test Mn/Ca variability at 2 cm depth, consistent with the
468 oxygen penetration depth at that station (Fig. 3). Moreover, the variability in Mn/Ca
469 values increases towards higher Mn/Ca values. This is in line with *M. barleeanus*
470 traveling more actively through the redox zones than *U. mediterranea* or *U. peregrina*.
471 Nitrate respiration could be mechanism allowing this dynamic behaviour by *M.*
472 *barleeanus* in the intermediate depth habitat. However, Pina-Ochao et al. (2010),
473 studying denitrification in foraminifera, reports nitrate storage in all three species
474 mentioned here. Notably, nitrate storage in *M. barleeanus* is lower than *U.*
475 *mediterranea* and *U. peregrina*. Alternatively *M. barleeanus* thrives in habitats with
476 varying oxygenation and hence also varying Mn levels, whereas the stable but high
477 Mn/Ca values in the Uvigerinids are related to their opportunistic behaviour.



478 With a redox-sensitive element such as Mn, in a dynamic geochemical
479 environment, it is not surprising that foraminifera exhibit high inter-individual
480 variability in their Mn/Ca incorporation. Benthic foraminifera reside in a 3D
481 geochemical mosaic, as reflected by a large spread of Mn values, in addition to
482 undergoing substantial temporal variability. Still, using Mn/Ca as a potential proxy
483 for redox conditions or primary productivity seems promising, as established
484 ecological characteristics of species are reflected by differences in Mn incorporation.
485 Apparently the large variability on both spatial and temporal scales averages out,
486 making Mn into a promising proxy for paleo-redox and organic matter flux.

487

488 **5. Conclusion**

489 This study investigates the link between benthic foraminiferal habitat preferences and
490 manganese incorporation in their tests. Manganese incorporation increases with
491 bottom-arriving labile organic matter content, driven by enhanced oxygen demand.
492 This results in a more shallow oxygen penetration depth with immediately below it
493 enhanced dissolved Mn levels. Shallow infaunal species calcify under lower
494 concentrations of Mn compared to intermediate infauna, in line with their depth
495 preference. Their depth habitat is related to in-sediment changes in redox conditions.
496 However, these distribution not necessarily vary synchronous with changes in redox
497 zonation as illustrated by the Mn/Ca variability in their tests (Fig. 8). The latter
498 reflects the Mn/Ca porewater composition, which itself is directly related to reactive
499 organic matter concentration and redox conditions. The foraminiferal Mn/Ca ratio and
500 inter-specimen variability, therefore, provides information on past Mn cycling within
501 the sediment. Consequently, the foraminiferal Mn/Ca ratio is a potential proxy for
502 bottom-water oxygenation and organic matter fluxes.



503

504 **Acknowledgements**

505 We thank captain and crew of the N/O Téthys 2 (CNRS-INSU) for their assistance
506 during the *BEHEMOTH* campaign. We acknowledge the technical assistance given by
507 Christine Barras, Mélissa Gaultier, Sophie Terrien and Gérard Chabaud from Angers
508 and Bordeaux University. We thank Serge Berné and Laetitia Maltese (Ifremer), for
509 providing us with maps of the study area and Xavier Durrieu de Madron (Perpignan
510 University) for discussions about water column structure. Helen de Waard (LA-ICP-
511 MS) and Karoliina Koho (SEM) (Utrecht University) are acknowledged for their
512 laboratory assistance. The Darwin Center for Biogeosciences provided partial funding
513 for this project. This paper contributes to the Netherlands Earth Systems Science
514 Center (NESSC –www.nessc.nl)

515

516 **References**

517 Accornero, A., Picon, P., De Bovée, F., Charrière, B., & Buscail, R.: Organic carbon
518 budget at the sediment–water interface on the Gulf of Lions continental margin.
519 *Continental Shelf Research*, 23(1), 79-92, 2003.
520
521 Alve, E., & Bernhard, J. M.: Vertical migratory response of benthic foraminifera to
522 controlled oxygen concentrations in an experimental mesocosm. *Oceanographic*
523 *Literature Review*, 9(42), 771, 1995.
524
525
526 Arndt, S., Jørgensen, B. B., LaRowe, D. E., Middelburg, J. J., Pancost, R. D. and
527 Regnier, P.: Quantifying the degradation of organic matter in marine sediments: A
528 review and synthesis, *Earth-Science Rev.*, 123, 53–86,
529 doi:10.1016/j.earscirev.2013.02.008, 2013.
530
531 Barnett, P. R. O., Watson, J. and Connely, D.: A multiple corer for taking virtually
532 undisturbed sample from shelf, bathyal and abyssal sediments, *Oceanologica Acta*, 7,
533 399-408, 1984.
534
535 Barras, C., Fontanier, C., Jorissen, F. and Hohenegger, J.: A comparison of spatial and
536 temporal variability of living benthic foraminiferal faunas at 550 m depth in the Bay
537 of Biscay, *Micropaleontology*, 56, 275-295, 2010.
538



- 539 Boyle, E. A.: Manganese carbonate overgrowths on foraminifera tests, *Geochim.*
540 *Cosmochim. Acta*, 47, 1815-1819, DOI: 10.1016/0016-7037(83)90029-7, 1983.
541
- 542 Burdige, D. J. and Gieskes, J. M. : A pore water/solid phase diagenetic model for
543 manganese in marine sediments. *American Journal of Science*, 283(1), 29-47, 1983.
544
- 545 De Lange, G. J.: Early diagenetic reactions in interbedded pelagic and turbiditic
546 sediments in the Nares Abyssal Plain (western North Atlantic): Consequences for the
547 composition of sediment and interstitial water, *Geochim. Cosmochim. Acta*, 50(12),
548 2543–2561, doi:10.1016/0016-7037(86)90209-7, 1986.
549
- 550 Elderfield, H., Yu, J., Anand, P., Kiefer, T. and Nyland, B.: Calibrations for benthic
551 foraminiferal Mg/Ca paleothermometry and the carbonate ion hypothesis, *Earth*
552 *Planet. Sci. Lett.*, 250(3–4), 633–649, doi:10.1016/j.epsl.2006.07.041, 2006.
553
- 554 Fontanier, C., Jorissen, F. J., Licari, L., Alexandre, A., Anschutz, P. and Carbonel, P.:
555 Live benthic foraminiferal faunas from the Bay of Biscay: faunal density, composition,
556 and microhabitats, *Deep Sea Research Part I: Oceanographic Research Papers*, 49,
557 751-785, DOI: 10.1016/S0967-0637(01)00078-4, 2002.
558
- 559 Fontanier, C., Jorissen, F. J., David, C., Anschutz, P., Chaillou, G. and Lafon, V.:
560 Seasonal and interannual variability of benthic foraminiferal faunas at 550m depth in
561 the Bay of Biscay. *Deep-Sea Research I*, 50, 457-494, 2003.
562
- 563 Fontanier, C., Mackensen, A., Jorissen, F. J., Anschutz, P., Licari, L., & Griveaud, C.:
564 Stable oxygen and carbon isotopes of live benthic foraminifera from the Bay of
565 Biscay: Microhabitat impact and seasonal variability. *Marine Micropaleontology*,
566 58(3), 159-183, 2006.
567
- 568 Fontanier, C., Jorissen, F. J., Lansard, B., Mouret, A., Buscail, R., Schmidt, S.,
569 Kerhervé, P., Buron, F., Zaragosi, S., Hunault, G., Ernout, E., Artero, C., Anschutz, P.
570 and Rabouille, C.: Live foraminifera from the open slope between Grand Rhône and
571 Petit Rhône Canyons (Gulf of Lions, NW Mediterranean), *Deep. Res. Part I Oceanogr.*
572 *Res. Pap.*, 55(11), 1532–1553, doi:10.1016/j.dsr.2008.07.003, 2008.
573
- 574 Froelich P. N., Klinkhammer G. P., Bender M. L., Luedtke N. A., Heath G. R., Cullen
575 D., Dauphin P., Hammond D., Hartman B. and Maynard V.: Early oxidation of
576 organic matter in pelagic sediments of the eastern equatorial Atlantic: suboxic
577 diagenesis. *Geochim. Cosmochim. Acta* 43(1075), 1090, 1979.
- 578 Glock, N., Eisenhauer, A., Liebetrau, V., Wiedenbeck, M., Hensen, C. and Nehrke,
579 G.: EMP and SIMS studies on Mn/Ca and Fe/Ca systematics in benthic foraminifera
580 from the Peruvian OMZ: A contribution to the identification of potential redox
581 proxies and the impact of cleaning protocols, *Biogeosciences*, 9(1), 341–359,
582 doi:10.5194/bg-9-341-2012, 2012.
583
- 584 Groeneveld, J. and Filipsson, H. L.: Mg/Ca and Mn/Ca ratios in benthic foraminifera:
585 the potential to reconstruct past variations in temperature and hypoxia in shelf regions,
586 *Biogeosciences*, 10(7), 5125–5138, doi:10.5194/bg-10-5125-2013, 2013.
587



- 588 Gross, O.: Influence of temperature, oxygen and food availability on the migrational
589 activity of bathyal benthic foraminifera: evidence by microcosm experiments. In *Life*
590 *at Interfaces and Under Extreme Conditions* (pp. 123-137). Springer Netherlands,
591 2000.
592
- 593 Hintz, C. J., Shaw, T. J., Chandler, G. T., Bernhard, J. M., McCorkle, D. C. and
594 Blanks, J. K.: Trace/minor element : calcium ratios in cultured benthic foraminifera.
595 Part I: Inter-species and inter-individual variability, *Geochim. Cosmochim. Acta*,
596 70(8), 1952–1963, doi:10.1016/j.gca.2005.12.018, 2006a.
597
- 598 Jochum, K. P., Weis, U., Stoll, B., Kuzmin, D., Yang, Q., Raczek, I., Jacob, D. E.,
599 Stracke, A., Birbaum, K., Frick, D. A., Gunther, D., Enzweiler, J.:
600 Determination of Reference Values for NIST SRM 610-617 Glasses Following ISO
601 Guidelines, *Geostandards and Geoanalytical Research*, 35, 4, 397-421, 2011.
602
- 603 Jorissen, F. J., de Stigter, H. C. and Widmark, J. G. V.: A conceptual model explaining
604 benthic foraminiferal microhabitats, *Mar. Micropaleontol.*, 26(1–4), 3–15,
605 doi:10.1016/0377-8398(95)00047-X, 1995.
606
- 607 Jorissen, F. J., Wittling, I., Peypouquet, J. P., Rabouille, C. and Relexans, J. C.: Live
608 benthic foraminiferal faunas off Cape Blanc, NW-Africa: Community structure and
609 microhabitats, *Deep Sea Research Part I: Oceanographic Research Papers*, 45, 2157-
610 2188, DOI: 10.1016/S0967-0637(98)00056-9, 1998.
611
- 612 Koho, K. A., Langezaal, A. M., van Lith, Y. A., Duijnste, I. A. P. and van der Zwaan,
613 G. J.: The influence of a simulated diatom bloom on deep-sea benthic foraminifera
614 and the activity of bacteria: A mesocosm study, *Deep. Res. Part I Oceanogr. Res. Pap.*,
615 55(5), 696–719, doi:10.1016/j.dsr.2008.02.003, 2008.
616
- 617 Koho, K. A., Piña-Ochoa, E., Geslin, E. and Risgaard-Petersen, N.: Vertical migration,
618 nitrate uptake and denitrification: Survival mechanisms of foraminifera
619 (*Globobulimina turgida*) under low oxygen conditions, *FEMS Microbiol. Ecol.*, 75(2),
620 273–283, doi:10.1111/j.1574-6941.2010.01010.x, 2011.
621
- 622 Koho, K. A., de Nooijer, L. J. and Reichart, G. J.: Combining benthic foraminiferal
623 ecology and shell Mn/Ca to deconvolve past bottom water oxygenation and
624 paleoproductivity, *Geochim. Cosmochim. Acta*, 165, 294–306,
625 doi:10.1016/j.gca.2015.06.003, 2015.
626
- 627 Koho, K. A., De Nooijer, L. J., Fontanier, C., Toyofuku, T., Oguri, K., Kitazato, H.
628 and Reichart, G. J.: Benthic foraminiferal Mn / Ca ratios reflect microhabitat
629 preferences, *Biogeosciences*, 14(12), 3067–3082, doi:10.5194/bg-14-3067-2017, 2017
630
- 631 Lea, D. and Boyle, E.: Barium content of benthic foraminifera controlled by bottom-
632 water composition, *Nature*, 338, 751-753, 1989.
633
- 634 Lewis, E., and Wallace, D. W. R.: Program Developed for CO₂ Systems Calculations.
635 ORNL/CDIAC-105, Carbon Dioxide Information Analysis Centre, Oak Ridge
636 National Laboratory U.S. Department of Energy, Oak Ridge, Tennessee, 1998.
637



- 638 Loubere, P., Meyers, P., and Gary, A.: Benthic foraminiferal microhabitat selection,
639 carbon isotope values, and association with larger animals: A test with *uvigerina*
640 *peregrina*, *Journal of Foraminiferal Research*, 25, 83-95. DOI:10.2113/gsjfr.25.1.83,
641 1995.
- 642
643 Mangini, A., Jung, M. and Laukenmann, S.: What do we learn from peaks of uranium
644 and of manganese in deep sea sediments?, *Mar. Geol.*, 177(1–2), 63,
645 doi:10.1016/S0025-3227(01)00124-4, 2001.
- 646
647 McKay, C. L., Groeneveld, J., Filipsson, H. L., Gallego-Torres, D., Whitehouse, M. J.,
648 Toyofuku, T. and Romero, O. E.: A comparison of benthic foraminiferal Mn / Ca and
649 sedimentary Mn / Al as proxies of relative bottom-water oxygenation in the low-
650 latitude NE Atlantic upwelling system, *Biogeosciences*, 12(18), 5415–5428,
651 doi:10.5194/bg-12-5415-2015, 2015.
- 652
653 Munsel, D., Kramar, U., Dissard, D., Nehrke, G., Berner, Z., Bijma, J., Reichart, G. J.
654 and Neumann, T.: Heavy metal incorporation in foraminiferal calcite: Results from
655 multi-element enrichment culture experiments with *Ammonia tepida*, *Biogeosciences*,
656 7(8), 2339–2350, doi:10.5194/bg-7-2339-2010, 2010.
- 657
658 Ní Fhlaithearta, S., Reichart, G.-J., Jorissen, F.J., Fontanier, C., Rohling, E.J.,
659 Thomson, J. & de Lange, G.J.: Reconstructing the seafloor environment during
660 sapropel formation using benthic foraminiferal trace metals, stable isotopes, and
661 sediment composition. *Paleoceanography*, 25(4), 2010. DOI:10.1029/2009PA001869
662
- 663 Ní Fhlaithearta, S., Ernst, S. R., Nierop, K. G. J., de Lange, G. J. and Reichart, G.-J.:
664 Molecular and isotopic composition of foraminiferal organic linings, *Mar.*
665 *Micropaleontol.*, 102, doi:10.1016/j.marmicro.2013.06.004, 2013.
- 666
667 Nürnberg, D., Bijma, J. and Hemleben, C.: Assessing the reliability of magnesium in
668 foraminiferal calcite as a proxy for water mass temperatures, *Geochim. Cosmochim.*
669 *Acta*, 60(5), 803–814, doi:10.1016/0016-7037(95)00446-7, 1996.
- 670
671 Pina-Ochoa, E., Hogslund, S., Geslin, E., Cedhagen, T., Revsbech, N. P., Nielsen, L.
672 P., Schweizer, M., Jorissen, F., Rysgaard, S. and Risgaard-Petersen, N.: Widespread
673 occurrence of nitrate storage and denitrification among Foraminifera and Gromiida,
674 *Proc. Natl. Acad. Sci.*, 107(3), 1148–1153, doi:10.1073/pnas.0908440107, 2010.
- 675
676 Reichart, G. J., Jorissen, F., Anschutz, P. and Mason, P. R. D.: Single foraminiferal
677 test chemistry records the marine environment, *Geology*, 31(4), 355–358,
678 doi:10.1130/0091-7613(2003)031<0355:SFTCRT>2.0.CO;2, 2003.
- 679
680 Risgaard-Petersen, N., Langezaal, A. M., Ingvarsdén, S., Schmid, M. C., Jetten, M. S.
681 M., Op Den Camp, H. J. M., Derksen, J. W. M., Piña-Ochoa, E., Eriksson, S. P.,
682 Nielsen, L. P., Revsbech, N. P., Cedhagen, T. and Van Der Zwaan, G. J.: Evidence for
683 complete denitrification in a benthic foraminifer, *Nature*, 443(7107), 93–96,
684 doi:10.1038/nature05070, 2006.
- 685
686 Rosenthal, Y., Morley, A., Barras, C., Katz, M. E., Jorissen, F., Reichart, G.-J., Oppo,
687 D. W. and Linsley, Braddock. K.: Temperature calibration of Mg/Ca ratios in the



- 688 intermediate water benthic foraminifera *Hyalinea Balthica*, *Geochem. Geophys.*
689 *Geosyst.*, 12(4), 2011. doi: 10.1029/2010GC003333
690
- 691 Schönfeld, J.: Benthic foraminifera and pore water oxygen profiles: A reassessment of
692 species boundary conditions at the Western Iberian margin, *Journal of Foraminiferal*
693 *Research*, 31, 86-107, 10.2113/0310086, 2001.
694
- 695 Schmiedel, G., Pfeilsticker, M., Hemleben, C., Mackensen, A.: Environmental and
696 biological effects on the stable isotope composition of recent deep-sea benthic
697 foraminifera from the western Mediterranean Sea *Mar. Micropaleontol.*, 51, 129–152
698 <http://dx.doi.org/10.1016/j.marmicro.2003.10.001>, 2004.
699
- 700 Van Cappellen, P. and Wang, Y.: Cycling of iron and manganese in surface
701 sediments: A general theory for the coupled transport and reaction of carbon, oxygen,
702 nitrogen, sulfur, iron, and manganese, *Am. J. Sci.*, 296(3), 197–243,
703 doi:10.2475/ajs.296.3.197, 1996.
704
- 705 Wang, Y. and Van Cappellen, P.: A multicomponent reactive transport model of early
706 diagenesis: Application to redox cycling in coastal marine sediments, *Geochim.*
707 *Cosmochim. Acta*, 60(16), 2993–3014, doi:10.1016/0016-7037(96)00140-8, 1996.
708
- 709 Wit, J. C., De Nooijer, L. J., Barras, C., Jorissen, F. J. and Reichart, G. J.: A
710 reappraisal of the vital effect in cultured benthic foraminifer *Bulimina marginata* on
711 Mg/Ca values: Assessing temperature uncertainty relationships, *Biogeosciences*, 9(9),
712 3693–3704, doi:10.5194/bg-9-3693-2012, 2012.
713
- 714 Yu, J. and Elderfield, H.: Benthic foraminiferal B/Ca ratios reflect deep water
715 carbonate saturation state, *Earth Planet. Sci. Lett.*, 258(1–2), 73–86,
716 doi:10.1016/j.epsl.2007.03.025, 2007.
717
718
719

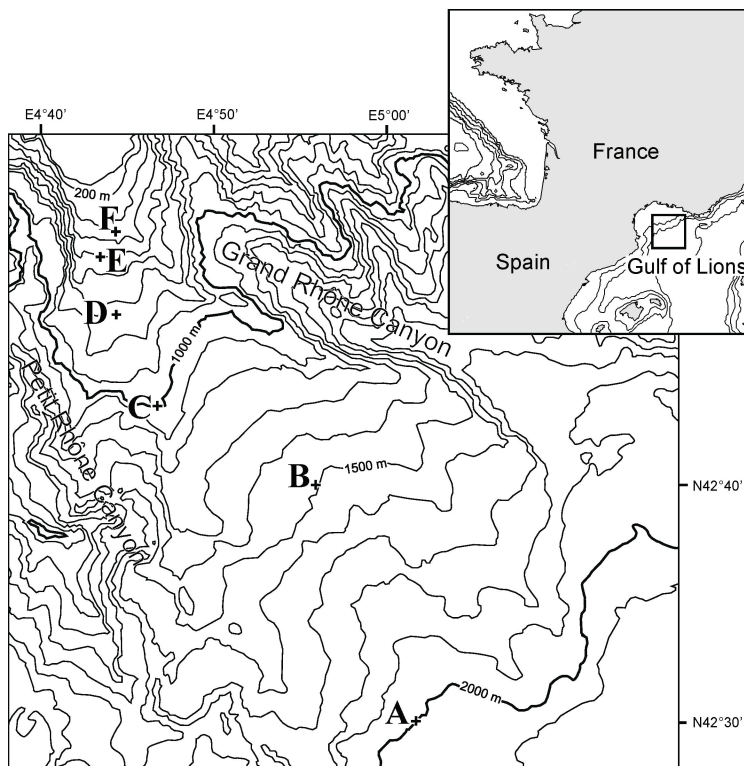


Figure 1. Location map showing sampling stations and bathymetry.

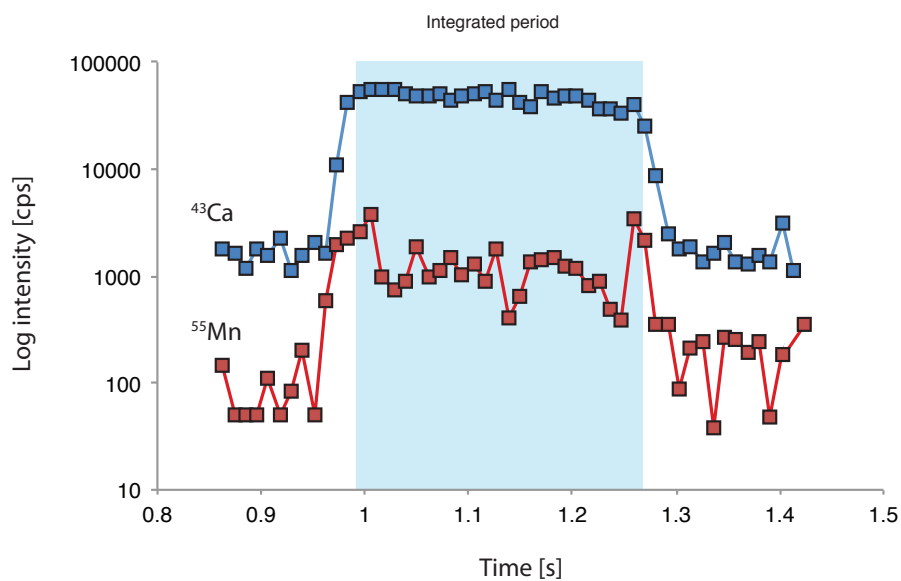


Figure 2. Example of a laser ablation profile, signal log intensity counts per second [cps] through time. The integrated signal is shaded.

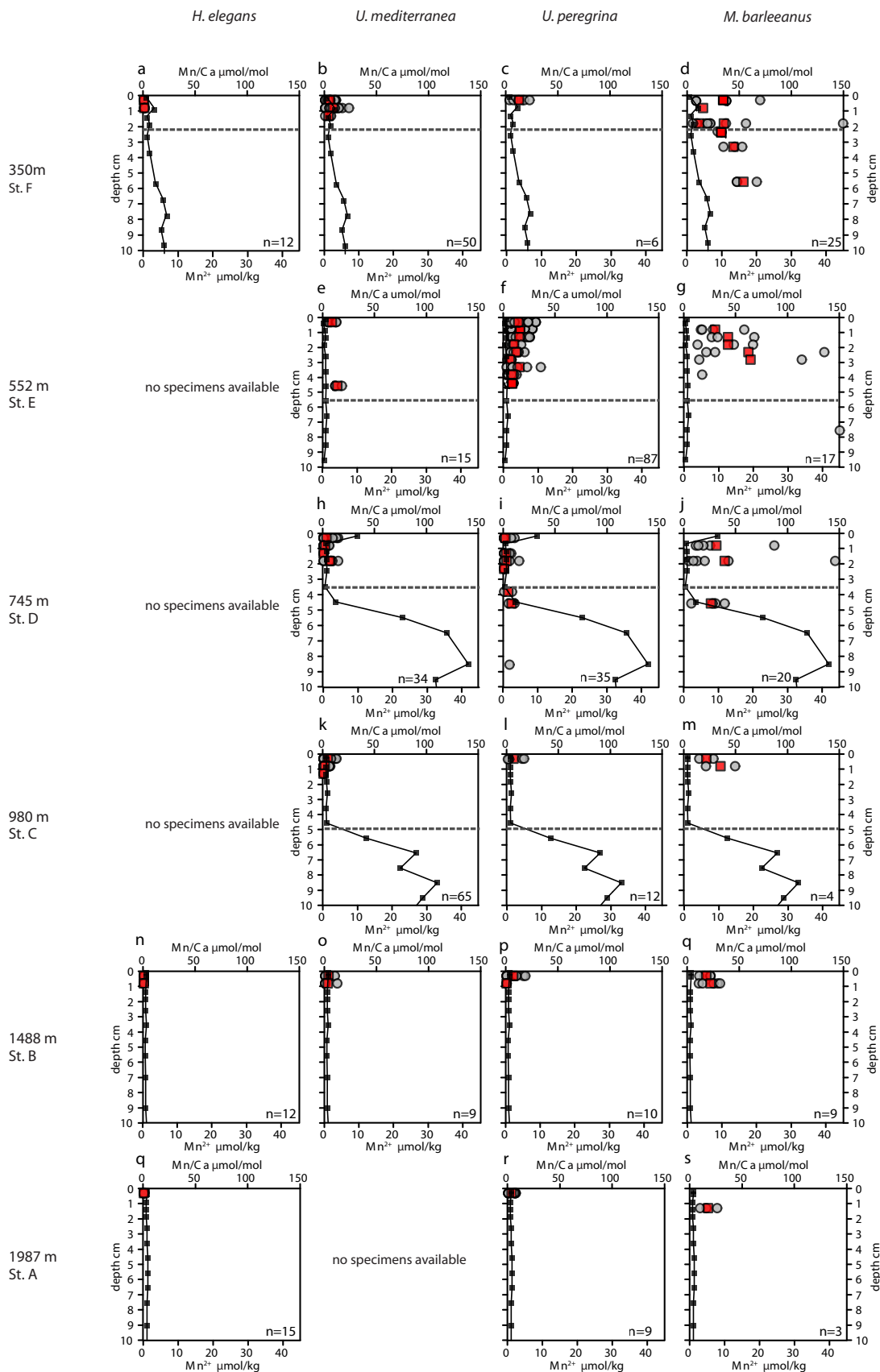


Figure 3. Plots of Mn/Ca (μmol/mol) measured in living (stained) *Hoeglundia elegans*, *Uvigerina mediterranea*, *Uvigerina peregrina* and *Melonis barleeanus*. Individual analyses are plotted (grey circles) alongside average values for a given depth in the sediment (red squares). Porewater Mn²⁺ (μmol/kg) profiles (black line) are plotted for all stations. The dashed grey line indicates the oxygen penetration depth (OPD).



Figure 4.

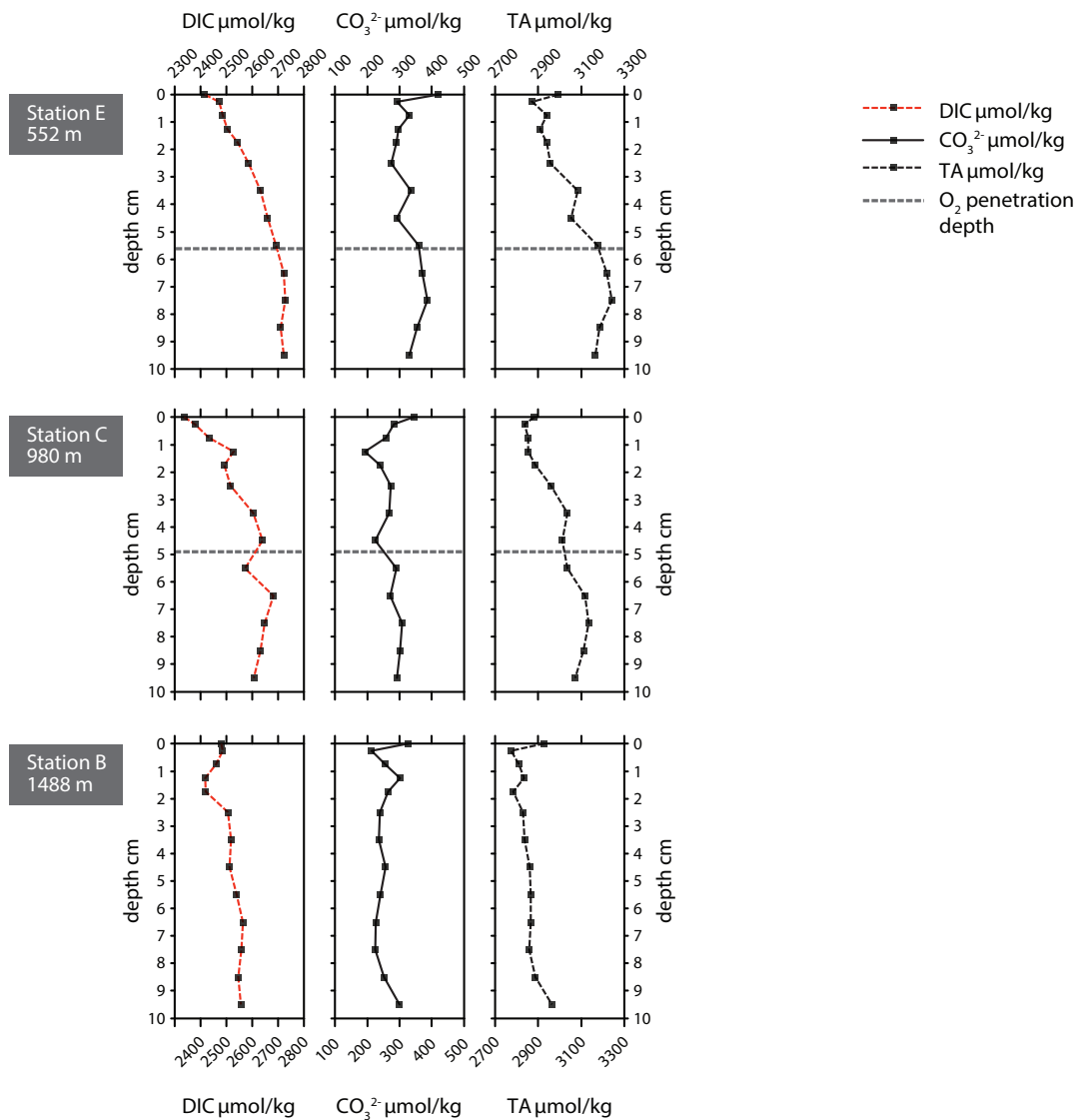


Figure 4. Carbonate chemistry parameters for stations E, C and B. A) Dissolved inorganic carbon (DIC), B) [CO_3^{2-}] in $\mu\text{mol/kg}$, C) Total alkalinity (TA) in $\mu\text{mol/kg}$.

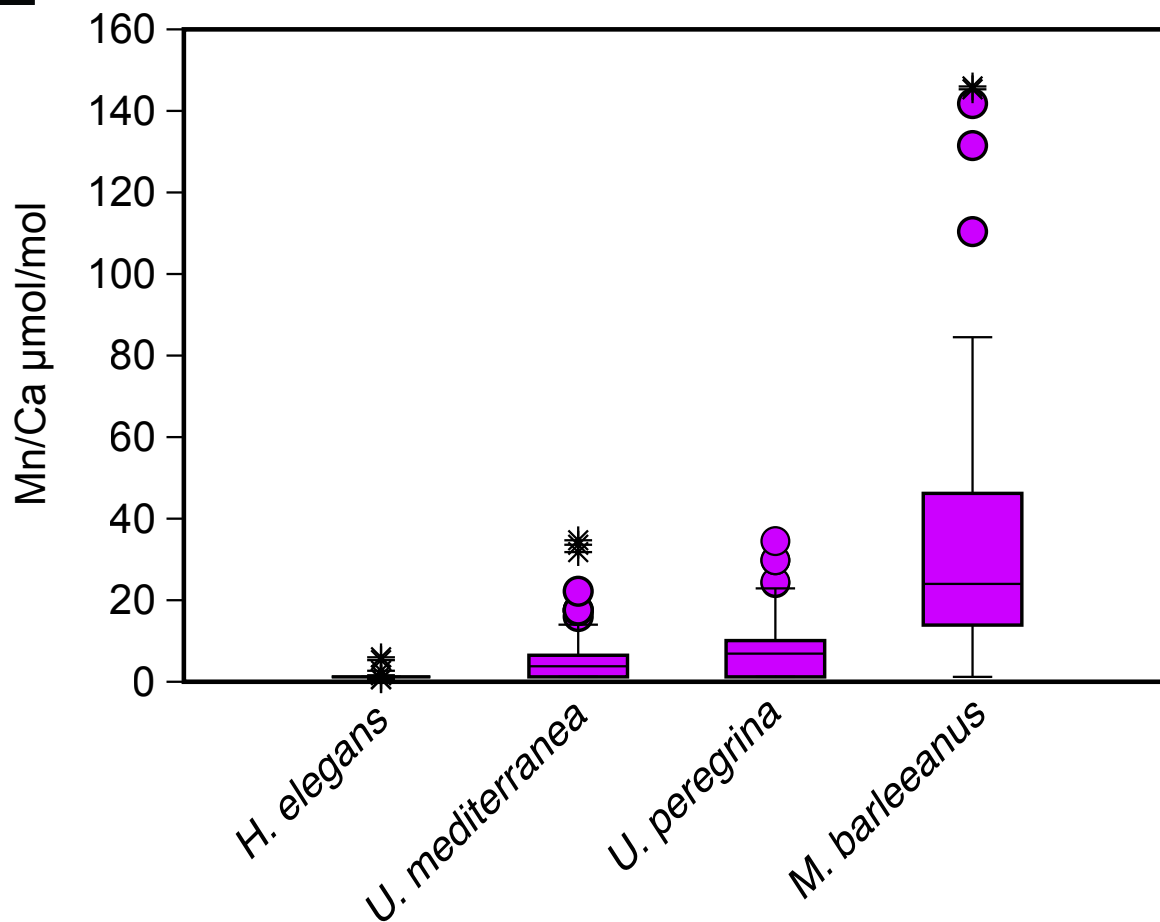


Figure 5. Box plots describing the distribution in Mn/Ca values measured in living (stained) individuals of *Hoeglundina elegans*, *Uvigerina mediterranea*, *Uvigerina peregrina* and *Melonis barleeanus*. The box represents all values between the 25th and 75th percentile. The dissection line through the box denotes the median. The whiskers are drawn from the top of the box up to the largest data point less than 1.5 times the box height from the box and similarly below the box. Values outside the whiskers are shown as circles, values further than 3 times the box height are denoted as stars.

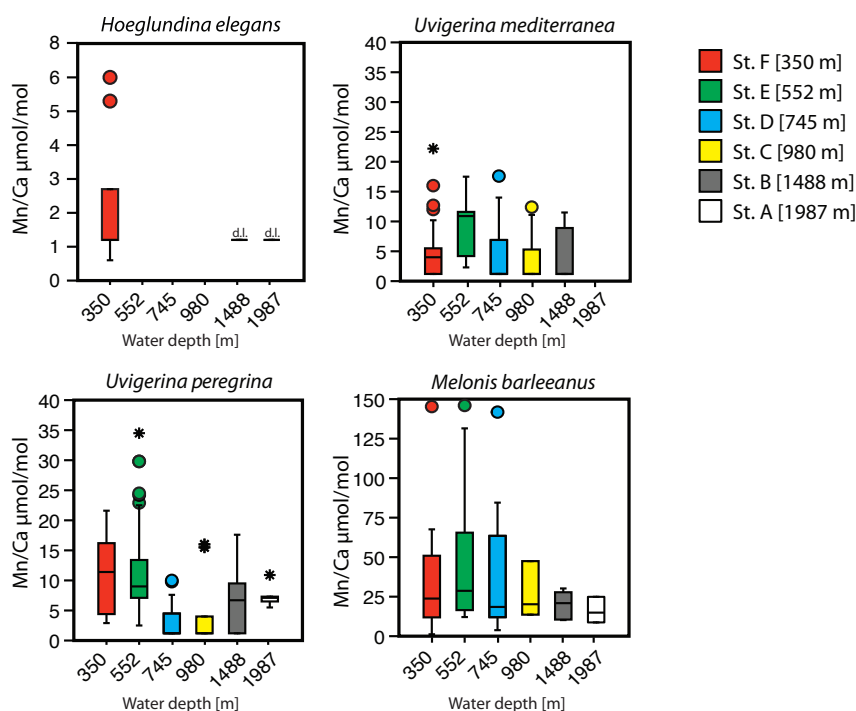


Figure 6. Box plots describing the distribution of Mn/Ca values across a depth transect (350–1987 m) measured in living (stained) individuals of *Hoeglundina elegans*, *Uvigerina mediterranea*, *Uvigerina peregrina* and *Melonis barleeanus*. Note that the scale of the y-axis varies. The box represents all values between the 25th and 75th percentile with the whiskers extending less than 1.5 times the box height. The dissection line through the box denotes the median. Values outside the whiskers are shown as circles, values further than 3 times the box height are denoted as stars.

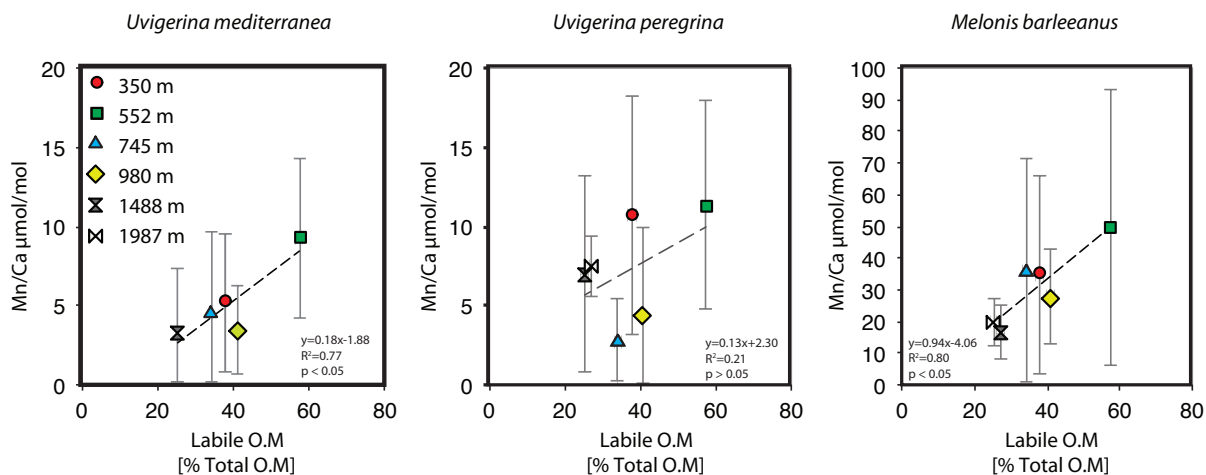


Figure 7. Plots of average Mn/Ca $\mu\text{mol/mol}$ versus labile organic matter [% Total Organic matter].

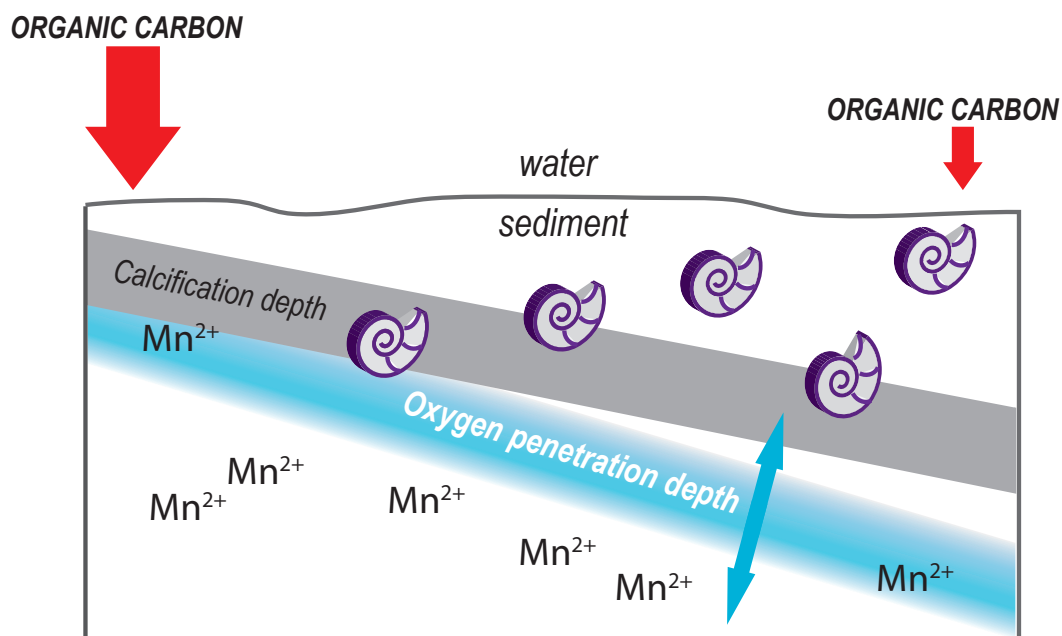


Figure 8. Schematic diagram of a shallow-infaunal and intermediate-infaunal benthic foraminifera and their spatial relationship with the sediment redox boundaries, migration zone, ALD and calcification depth.



Table 1. Water depth, coordinates and bottom water physio-chemical parameters: Temperature ($^{\circ}\text{C}$), salinity, and oxygen penetration depth (mm) for six stations F-A. (* Xavier Durrieu de Madron, Pers. Comm.)

Station	Depth (m)	Latitude (N)	Longitude (E)	Bottom water temperature* ($^{\circ}\text{C}$)	Bottom water salinity *	Oxygen penetration depth (mm)
F	350	42 $^{\circ}$ 52'32	4 $^{\circ}$ 42'43	13.2	~38.5	20.5 \pm 3.3
E	552	42 $^{\circ}$ 48'78	4 $^{\circ}$ 43'21	13.2	~38.5	57.2 \pm 4.5
D	745	42 $^{\circ}$ 46'66	4 $^{\circ}$ 43'91	13.1	~38.5	36.5 \pm 1.6
C	980	42 $^{\circ}$ 43'18	4 $^{\circ}$ 46'58	13.1	~38.48	50.7 \pm 6.3
B	1488	42 $^{\circ}$ 38'83	4 $^{\circ}$ 56'03	13.1	~38.46	141.5 \pm 0.0
A	1987	42 $^{\circ}$ 28'25	5 $^{\circ}$ 00'61	13.1	~38.46	197.0 \pm 11.0



Table 2. Number of LA-ICP-MS analyses per benthic foraminifera species per sample per station.

Station	Depth (m)	Sample intervals (cm)	<i>Hoeglundina elegans</i> no. analyses	<i>Uvigerina mediterranea</i> no. analyses	<i>Uvigerina peregrina</i> no. analyses	<i>Melonis barleeanus</i> no. analyses
F	350	0-0.5	2	18	5	1
		0.5-1	4	13		2
		1-1.5		3		
		1.5-2				10
		2-2.5	1			2
		3-3.5				3
		5-6				3
E	552	0-0.5		5	26	
		0.5-1			9	4
		1-1.5			14	3
		1.5-2			5	3
		2-2.5			7	3
		2.5-3			6	2
		3-3.5			6	
		3.5-4			8	1
		4-5			3	
7-8					1	
D	745	0-0.5		20	13	
		0.5-1		6		5
		1-1.5		3	6	
		1.5-2		7	8	6
		2-2.5			4	
		3.5-4			2	
		4-5			2	4
		8-9			2	
C	980	0-0.5		20		2
		0.5-1		20		2
		1-1.5		4		
B	1488	0-0.5	3	4	10	4
		0.5-1	9	5	3	5
A	1987	0-0.5	15		10	
		1-1.5				3



Table 3. Descriptive statistics (minimum, maximum, mean, median, standard deviation and interval of maximum frequency of total analyses for *H. elegans*, *U. mediterranea*, *U. peregrina* and *M. barleeanus* for Mn/Ca $\mu\text{mol/mol}$.

Mn/Ca $\mu\text{mol/mol}$	<i>H. elegans</i>	<i>U. mediterranea</i>	<i>U. peregrina</i>	<i>M. barleeanus</i>
Min	dl*	dl*	dl*	3.91
Max	0.69	22.71	35.38	149.50
Mean	0.04	4.03	8.28	37.22
Median	dl*	1.04	7.45	24.76
Std. deviation	0.16	5.03	7.17	35.17
Max. frequency interval	dl-7.50 (100% < 1)	dl-7.50 (80%)	dl-7.50 (53%)	7.5-15 (23%)



Table 4. Relative standard deviation (% RSD) of intra-individual values in Mn/Ca within four species of benthic foraminifera (*H. elegans*, *U. mediterranea*, *U. peregrina* and *M. barleeanus*).

Element	<i>H. elegans</i> % RSD	<i>U. mediterranea</i> % RSD	<i>U. peregrina</i> % RSD	<i>M. barleeanus</i> % RSD
Mn	21	23	20	51



Table 5. Relative standard deviation (% RSD) of inter-individual values in Mn/Ca within four species of benthic foraminifera (*H. elegans*, *U. mediterranea*, *U. peregrina* and *M. barleeanus*).

Element	<i>H. elegans</i> % RSD	<i>U. mediterranea</i> % RSD	<i>U. peregrina</i> % RSD	<i>M. barleeanus</i> % RSD
Mn	400	125	87	97



Table 6. Manganese porewater – carbonate partition coefficient for foraminiferal species *Uvigerina mediterranea*, *Uvigerina peregrina* and *Melonis barleeanus*.

Station	Partition coefficient (D) ¹		
	<i>U. mediterranea</i>	<i>U. peregrina</i>	<i>M. barleeanus</i>
E (552 m)	1.7	1.8	7.0
C (980 m)	1.2	-	5.1
B (1488 m)	2.2	2.3	4.1

¹Porewater-carbonate partition coefficients were calculated using the average porewater Mn/Ca [$\mu\text{mol/mol}$] measured above the oxygen penetration depth and the average carbonate Mn/Ca [$\mu\text{mol/mol}$] measured in *U. mediterranea*, *U. peregrina* and *M. barleeanus*, for all specimens recovered above the reported oxygen penetration depth (Fontanier et al., 2008).